Vol. XVI—No. 4 December 1971

The SPEX Speaker

INDUSTRIES, INC. · 3880 PARK AVENUE · METUCHEN, N.J.,08840 · ☎(201)-549-7144

MATRIX ISOLATION LASER RAMAN SPECTROSCOPY AT CRYOGENIC TEMPERATURES

G.A. Ozin

Lash Miller Chemical Laboratories, and Erindale College,

University of Toronto, Toronto 181, Ontario, Canada.

TWO basic approaches to the study of short-lived chemical species have been devised. One involves rapid observation usually but not necessarily in the gas phase. For example, the technique of flash photolysis requires a repetitive, high-intensity, short-duration flash lamp and a suitably gated spectrometer which is opened to the substance under study for a fleeting moment immediately after each flash. In the other method the short-lived species is immobilized at cryogenic temperatures. Greatly diluted in an inert, host matrix to keep its molecules from reacting with themselves, the substance is trapped at 4.2K, there preserved for analysis. When highly reactive, short-lived species are so constrained, guest-guest as well as host-guest reactions are minimized.

The number and types of problems encountered in the spectroscopy of low temperature matrices are considerable. This paper will be concerned with the production and stabilization by trapping of highly reactive inorganic species in rigid matrices at low temperatures and their subsequent analysis by laser Raman spectroscopy. The contents derive largely from our own experiences which, in turn, are based on the excellent groundwork laid by others [1]. Not considered here are the Raman spectra of isolated species in either clathrates or doped alkali-halide matrices, both of which do not generally require cryogenic conditions.

The need for reliable Raman data to complement matrix infrared data is obvious, for example, to aid in the indentification of new species and for making reliable structural and vibrational assignments for either new chemical systems or for systems whose available data has otherwise remained incomplete or ambiguous.

The intricacies of experimental procedures in the Raman spectroscopy of matrix-isolated species generally differ from those in the infrared and, in the hope of presenting this new technique as clearly as possible, the paper has been divided into seven sections:

1. The matrix isolation technique
2. Properties of the matrix host and guest
3. Techniques for generating reactive species
4. The advantages and limitations of the matrix Raman technique
5. Matrix Raman cryogenic techniques
6. Recent matrix Raman results
7. Raman depolarization measurements for matrix isolated species using the Cold Gas Model.

AS early as 1885 Widemann and in 1901 Dewar [2] noted that complex molecules phosphoresce when irradiated at low temperatures. Presumably, they had trapped an unstable, reactive species and, in so doing, had inadvertently discovered the matrix isolation technique. Vergard [3] in 1924 studied the luminescence from solid N_2 at 21K after electron bombardment. Lewis and Lipkin[4] in 1942, photolyzing organic molecules suspended in rigid glassy media at 77K and 20K, succeeded in producing stable radicals in the hydrocarbon glass.

The modern phase of study began in 1951 when Rice and Freamo [5] reported a blue paramagnetic substance on condensing at 77K the products of HN_3 which had been passed through a glow discharge. In 1954 researchers in seven laboratories independently reported their attempts to detect free radicals suspended in a rigid, inert matrix [6]. Analytical methods applied included ESR, IR, UV-visible spectroscopy, magnetic susceptibility, and calorimetry.

Norman and Porter [7], and independently Whittle, Dows and Pimentel [8] proposed what is now called the matrix isolation method for studying free radicals or highly reactive molecules. Pimentel [9] was the first to report the detection, by infrared spectroscopy, of a free radical suspended in a CO matrix support ($HI + CO \xrightarrow{h\nu} HCO$) and was first to place the matrix technique on a semiquantitative basis [10]. He selected various matrix supports as typical of strongly hydrogen-bonded solutes (HCl, H_2O, NH_3, etc.) and for each determined the matrix-to-solute ratios (M/A) and temperatures for which efficient isolation could be achieved.

Molecular beam evaporation from a Knudsen cell as a source of new chemical species for matrix isolation study was first suggested by Pimentel [10]. Following this lead, Linevsky [11] showed that many of the difficulties of high-temperature infrared work, such as interfering reactions with furnace walls, complexity of spectra caused by hot bands, and difficulty of achieving a sufficiently high concentration for a long period of

time, could be reduced or eliminated by matrix trapping. Weltner's [12] elegant work on matrix-isolated C_2, C_3, C_4, etc., in which carbon was vaporized at approximately 2700C and co-condensed with a matrix gas at 4.2K, stands out as an impressive example of the versatility of the technique.

INERT gases are usually chosen as matrix materials because of their low lattice energies. Any interactions between host atoms or molecules are weak, as are the host-guest interactions. Thus, optical properties of the guest remain characteristic of the free guest molecule with only slight perturbation by the matrix. These are referred to as "matrix shifts" and are usually small (less than 20 cm^{-1}) for non-polar species. Matrix-to-guest ratios are usually kept very high to minimize guest-guest interactions. Splitting of a spectral line caused by guest-guest interactions in nearest or next nearest sites in the host matrix can ordinarily be prevented by decreasing the concentration of the guest species. Splittings of bands may also arise from different orientations of the guest species in the surrounding host cage or from the different environments experienced by a guest species when trapped in different sites in the host lattice (for example, interstitial, substitutional or defect sites). Such splittings can usually be identified by changing matrix materials.

The guest environment depends on the conditions of matrix preparation but is found to be nearly always of a randomly oriented nature. This makes possible the measurement of depolarization ratios for the Raman spectra of matrix isolated species [13, 14]. Occasionally, however, preferential orientation of certain species in the matrix does occur. For example, matrix infrared measurements have revealed that for certain planar monomers, orientation parallel to the target material is favored [15]. This would make possible the measurement of matrix Raman polarization data for a molecule in a space-fixed coordinate system but in a gas-like environment. In principle such data could serve to test the "oriented gas-phase approximation" which was originally devised as a means of interpreting single crystal data for molecular crystals [16].

Apart from a role in inhibiting reactions, low temperatures also simplify spectra by preventing vibrational transitions from any but the lowest levels and by eliminating "hot bands." At low temperatures, rotational excitations are suppressed as well, and as the integrated intensity of the absorption or scattering remains the same, the effect is to sharpen IR or Raman lines. At the same time quenching of the rotational structure serves to sharpen the vibrational lines thereby facilitating their interpretation. One disadvantage of the absence of rotational lines is the loss of a means of designating symmetry species from vibration-rotation band envelopes. However, band sharpening usually means that nearby weaker fundamentals and isotopic structure can usually be resolved.

Diffusion considerations are of prime importance in the initial preparation of the matrix. The rate of diffusion is usually experimentally insignificant at 4.2-20K. This is important because uncontrolled diffusion leading to reaction and aggregation is undesirable. On the other hand, controlled diffusion can be advantageous. For example, careful annealing of the matrix may improve the perfection of the lattice structure and so remove multiple-site effects, reduce undesirable scattering by improving the transparancy of the matrix, etc. Short-range diffusion can be put to work to produce radicals by *in situ* photolysis or chemical reactions.

In any matrix isolation study it is important to distinguish bands due to higher aggregates from those due to efficiently isolated monomeric species. One way to do this is to vary the matrix-to-guest ratio. Another involves the spectroscopic observation of the polymerization or reaction of the monomeric species by performing a diffusion-controlled warm-up experiment. Thus, matrix materials such as Ar or N_2 are rigid below 20K but become soft at 30K to permit long-range diffusion and reaction of the trapped species within the matrix. Intensity variations of spectral lines arising from separate species in the matrix at the onset of and during the course of a reaction will usually behave similarly so their growth or decay plots become an aid toward vibrational assignment.

Fateley's "blanket effect" [17] was a term introduced to describe the upper limit of the rate of deposition set by the thermal stability of the species sought. Too rapid a deposition may cause a flood of liberated energy by the condensing gas which may alter or completely destroy delicate molecules. Two variants of the blanket effect should be distinguished: An internal blanket describes the undesirable release of energy and is inherent in every system. An external blanket occurs when an operator deliberately covers a film under study with a burst of matrix gas to see how this release of energy will affect the spectrum.

Efficient isolation depends on a high ratio of matrix gas to trapped species and very slow depositions over many hours. Such long deposition times are understandably inconvenient (although the recently developed closed cycle helium refrigerators alleviate this problem) and Rochkind's pulsed technique [18] could prove to be very helpful in this respect. In this technique, the gaseous mixture is deposited in a series of short, controlled bursts; for reasons not completely understood, it produces better guest spectra than when the mixture is deposited more slowly. Thus far, the technique has not been applied to highly reactive species.

The need for liquid helium or hydrogen temperatures, especially in laser-excited, matrix Raman work is of primary importance. Ne, Ar, Kr, Xe and N_2 have generally been selected as matrix supports although reactive matrices such as O_2, CO, SF_6, CO_2, C_6H_{12}, $SiMe_4$, etc. are also finding application. With the latter, reaction of the guest species and the matrix material may readily be followed spectroscopically at the onset of a diffusion-controlled reaction.

IT is appropriate to divide the many different methods of generation of reactive species into two broad categories:

1. Generation at ambient or high temperatures in the gas phase and then rapid quenching with excess inert gas;
2. Generation *in situ* in the matrix.

Techniques employed for the production of unstable species are mostly classical. A selection of representative but not exhaustive examples is listed below:

1. Direct trapping from the vapor phase e.g. volatile hydrogen bonded species [20], H_2O, NH_3, CH_3OH, HCl, HN_3

2. High-temperature, molecular-beam condensations e.g. Li_2F_2 [21], B_2O_3 [22], C_3 [23], $NaAlF_4$ [24]
3. Hot-tube pyrolysis prior to deposition to form CH_3 [25].
4. High-temperature metal atom-molecule cocondensations to form Li and CCl_3 [26]; LiON [27]; O_2RbO_2 [28]; $Pd(CO)_n$ where n = 1-4 [76].
5. Double furnace metal-metal-molecule cocondensations to form KO_2Rb [28].
6. High-temperature, gas-flow Knudsen cell reaction techniques to form $GeCl_2$ (monomer) [29]; $NiCl_2$ (monomer) [30].
7. Microwave or electrical discharge techniques to form HBr_2 [31]; Cl_3 [32].
8. Generation *in situ* by primary photolysis to form OF and F [33]; FN and N_2 [34]; $Ni(CO)_2$ [35].
9. Generation *in situ* by primary photolysis and reaction to form CO_3 and O_2 [36]; KrF_2 [37]; O_2F_2 and O_2F [38].
10. Generation *in situ* by alkali metal-atom photoionization to form SO_2^- [39].

PRIMARY reasons for the slow development of matrix Raman spectroscopy include:

(a) In the pre-laser period of Raman spectroscopy, severe limitations were imposed by mercury arc excitation. Generally speaking, one was restricted to the study of colorless or pale yellow matrices, the most suited of which were crystalline rather than opaque. Also, sample handling under cryogenic conditions was experimentally difficult.

(b) The introduction of lasers to Raman spectroscopy was especially advantageous in low-temperature studies. Even so, the inherent weakness of the Raman effect (approximately 10^{-6} of the intensity of the Rayleigh scattering) and the need to work at A/M concentrations of less than 1% for efficient isolation (often with high background scattering) has undoubtedly limited the advancement of matrix Raman spectroscopy.

Some advantages of the matrix Raman technique are:

(a) The complete vibrational spectroscopic range ($\sim$ 30-3500 cm^{-1}) can be covered in one scan without the need for changing window materials, matrix supports or spectrometer optics.

(b) Vibrational and structural information may often be directly obtained from the frequencies of totally symmetrical Raman-active stretching modes without the requirement of detailed analysis. Usually, producing the strongest and sharpest bands in the Raman spectrum, totally symmetrical modes are easily identified.

(c) Polarization measurements are easily made and, in principle, depolarization ratios may be obtained for species randomly oriented in the host matrix. Also the possibility of obtaining matrix Raman polarization data for molecules oriented in the host matrix may be realized.

(d) Different areas of the matrix can be monitored by scanning the laser beam over the surface of the matrix. In this way one can check the uniformity of the matrix and investigate areas for differing degrees of isolation.

(e) Gas-phase Raman data, not readily accessible because of the high temperatures (>1000C) required to attain the necessary vapor pressures (usually >100 Torr) may be obtained by high-temperature molecular-beam techniques (where low vapor pressures of material are a prerequisite of successful isolation) and subsequent quenching at low temperatures in a matrix diluent.

(f) Raman spectroscopy in a matrix environment is not normally feasible in the gas phase because resonance fluorescence phenomena often dominate and obliterate vapor phase Raman spectra.

Six main factors may limit the success and applicability of matrix isolation laser Raman spectroscopy:

(a) The Matrix Solute Concentration Limit

We have been able to detect 1 part of solute in 10,000 of a matrix under favorable conditions although matrix-to-solute ratios of more than 1000:1 are not generally accessible with conventional detection techniques. However, ratios of about 500-100:1 are often sufficient to obtain successful isolation as evidenced by the absence of solute lattice modes, removal of crystal field effects and observation of a monomer which polymerizes on the onset diffusion.

Before we set out on our program of matrix isolation Raman spectroscopy it was necessary to ascertain the approximate concentration limits of the technique. This was achieved by studying stable species such as CS_2, SF_6, $CHCl_3$, SO_2, S_2Cl_2, Cl_2, etc. in various matrix supports at low solute concentrations. Compared with IR, the detection capabilities of laser Raman spectroscopy were found to be very encouraging. For CS_2, we were able to record a matrix Raman spectrum of reasonable quality (Fig. 1) at a M/A = 10,000:1. The results indicated that as little as 1 ppm of CS_2 in CO_2 could probably be detected. A second rather stringent test was to detect the extremely weak lines of ν_1 of CS_2 corresponding to the very low abundance combination of ^{33}S and ^{34}S isotopic species.

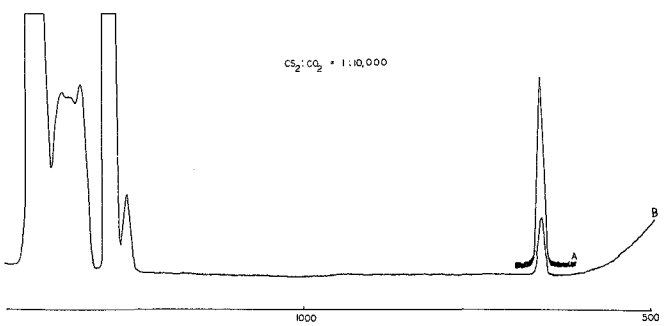

Fig. 1. The matrix Raman spectrum of CS_2 in CO_2 at M/A = 10,000:1 and a temperature of 4.2K. A is a higher sensitivity scale than B.

Even though these particular choices of matrix-isolated molecules represent favorable cases, in that many are inherently strong Raman scatterers, the results were nevertheless significant as they ranged within the concentration required for efficient isolation (approximately 0.1-1%).

(b) Color of the Solute or Matrix

A serious obstacle in working with highly reactive species is absorption of the laser light which will cause local heating in the matrix material. Subsequent reduction in the rigidity of the matrix may be sufficient to destroy the delicate species under investigation. Softening effects are easily recognized by sudden increases in pen noise, reduction in signal intensity and baseline variations. Often the result of absorption of the laser beam by the sample can be seen visually as a hole or burn in the matrix. Local heating effects may sometimes be avoided by working with a defocused, or line focused laser beam but with corresponding loss of signal intensity. Additionally, local heating may be reduced by careful selection of the laser exciting wavelength. Dye lasers, with their continuous range of color, may prove a boon.

(c) Power Output of the Laser

In all matrix isolation Raman experiments, particularly of reactive species, it is of prime importance initially to scan the spectrum at the lowest possible laser energy to obtain any signal, however poor. In this way, a minimum of energy is dissipated in the matrix and, as a result, any temperature rise can be kept to a minimum. Once the desired Raman spectrum has been obtained, spectral scans can be repeated at gradually increasing laser intensity. Any changes observed in the Raman spectra on repeat scans can then be attributed to diffusion and reaction in the matrix. This laser method of initiating self-diffusion in the matrix may prove to be a bonus of the laser Raman technique.

(d) Resolution

High-resolution Raman spectroscopy will invariably be difficult to achieve for matrix isolated species. The low concentration required for efficient isolation will result in a weak Raman spectrum and to achieve an acceptable signal-to-noise ratio, large spectral slit widths become necessary. How good a resolution can be achieved is intimately related to the light scattering properties of the matrix and the degree of sophistication of the entire Raman system.

(e) Light Scattering Properties of the Matrix

Background scattering is extremely sensitive to the physical nature of the matrix. The amount of background scattering may be reduced and, the quality of the spectra correspondingly enhanced by experimenting with different types of matrices and by recording spectra at different angles of incidence of the laser beam on the matrix. Excitation at near-grazing incidence rather than the customary 45-60° can frequently reduce the background scattering and so allow closer approach to the exciting line and simultaneously improve the signal-to-noise.

The most favorable matrix for Raman spectroscopy is one that is transparent and deposited on a highly polished mirror surface (platinum, silver and copper). This arrangement generally produces lowest background scattering with lowest noise level and is particularly well suited for recording polarization data.

(f) Fluorescence Problems in Matrix Raman Spectroscopy

Many of the fluorescence problems which plagued early Raman studies with mercury arc excitation are either eliminated or substantially reduced with laser excitation. However, when studying very dilute matrices by laser Raman spectroscopy extremely high gains are required, with the result that trace quantities of fluorescent impurities can cause serious spectral interference for certain exciting wavelengths. High vacuum grease, diffusion pump oils or other impurities (cryopumped into the matrix or carried to the tip with the matrix gas) can play havoc with results and must be avoided.

Apart from foreign contaminants, there is also the possibility of intense fluorescence from the matrix isolated species itself. With luck, such fluorescence may be eliminated by changing to a different laser exciting wavelength.

ALTHOUGH "home made" glass helium dewars provide an economical route to matrix Raman experiments, they are invariably fragile, difficult to handle and costly in terms of liquid helium consumption. The recently developed and commercially available (Air Products and Chemicals, Inc.) liquid helium-transfer Cryo-Tip systems and closed-cycle helium refrigerators, are more convenient. Flexible transfer lines allow complete maneuverability of the cold end and the design permits its independent rotation with respect to the vacuum shroud during operation. Temperature control of the cold tip is also easily achieved by a combination of needle valves and a heating element.

The arrangement employed in our laboratory, completely portable and vibration-free, is shown in Fig. 2. It is incorporated into a three-axis, universal stage to facilitate optimization of signal intensity and the reproducible scanning and recording of various areas of the matrix. For the study of matrix Raman spectra of molecules at high temperature, we have mated a cold tip to a furnace as shown in Fig. 3. The arrangement consists basically of a copper or silver cold tip on which the matrix and molecular beam are condensed, and a Knudsen cell to generate the molecular beam. The matrix gas and the molecular beam are cocondensed simultaneously on the cold tip with the matrix gas sufficiently in excess to isolate the molecules effusing from the cell.

When working with dilute matrices and Ne, Ar, Kr and Xe as matrix supports, one is faced with the initial problem of lining up the matrix with respect to the spectrometer to obtain an optimum signal. This can present a major problem because, as a rule, the Raman signal is very weak. By choosing a matrix support which itself gives rise to a strong Raman spectrum, one can optimize the solute Raman signal by maximizing the spectrum of the support. In such circumstances efficient scatterers such as N_2, O_2, CO, CO_2, SF_6, $SiMe_4$, etc., serve a double function.

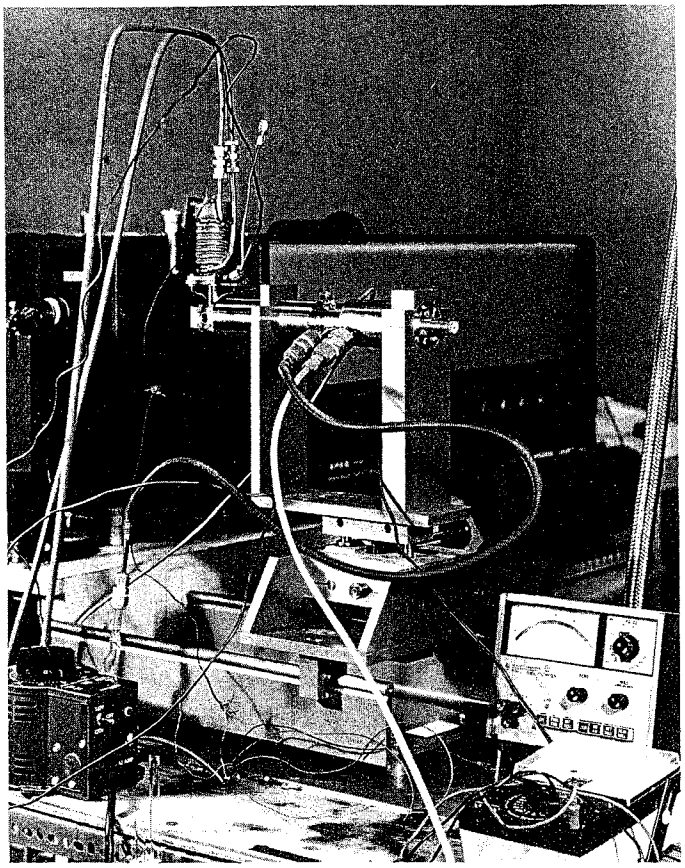

Fig. 2. At the University of Toronto, the sample matrix is prepared in a Cryo-Tip assembly and then moved into the illumination-collection system adjoining a Spex 1401 Double Spectrometer.

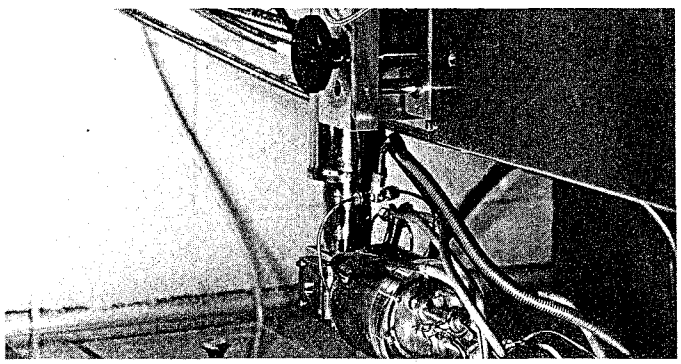

Fig. 3. In 1962, Weltner pioneered the development of furnace-refrigeration combinations where the temperature over a distance of a few cm plunges from as high as 3000K to as low as 4.2K. In our design, the sample is loaded into an evacuated Knudsen cell. This is a resistance-heated metal or graphite tube about ½ cm diameter by 3 cm long. Through a tiny hole drilled in the cylinder wall, the gaseous sample streams out as a molecular beam. After passing through radiation shields, it strikes and condenses on the cold tip together with the matrix gas which is generated separately.

SOME reactive species which have recently been stabilized by trapping the products of a microwave discharge and identified by matrix infrared spectroscopy are HCl_2 [40], HBr_2 [31], Cl_3 [32], $XeCl_2$ [41], etc. We have successfully employed the matrix Raman technique for studying similar types of reactions as illustrated by Br_3 [42], Br_4 [43], $XeCl_2$ [44], KrF_2 [45], SiF_3 [45], etc. Because of the poor selectivity of microwave discharges, their applications to matrix isolation studies are limited to simple systems.

Once thought impossible to produce, Xenon dichloride has gradually lost its allure. Since its identification in 1966 by mass spectroscopy [47] and by matrix isolation infrared spectroscopy [41] structural and chemical studies of $XeCl_2$ have essentially been discontinued. However, a structural ambiguity remains. It relates to the fact that its centrosymmetric linear assignment is based solely on the infrared observation of the anti-symmetric stretching mode which was observed at 313 cm^{-1}. The infrared active Xe-Cl deformational mode was not observed as it was expected to lie below the low frequency limit of the spectrometer.

We have now unambiguously assigned the molecular structure of $XeCl_2$ by observation of its matrix Raman spectrum. From the earlier IR data the molecule could have had either a linear or bent geometry. The former would be centro-symmetric ($D_{\infty h}$) showing only one strong line Σg^+ in the xenon-chlorine stretching region; the latter, with two planes of vertical symmetry (C_{2v}) would show one strong and one weak xenon-chlorine stretching mode ($a_1 + b_2$) as well as a lower frequency deformational mode (a_1).

Relying on methods developed by previous experimentalists for the production of matrix-isolated $XeCl_2$, we observed the matrix Raman spectrum shown in Fig. 4 [44]. A strong single line appeared at 253 cm^{-1} proving the linear geometry.

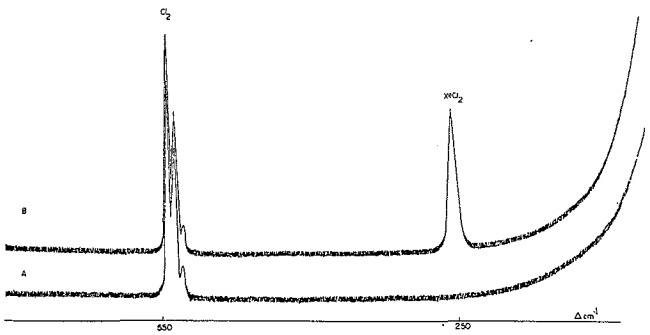

Fig. 4. The Raman spectra of a xenon-chlorine (25:1) matrix at 4.2K showing it to be unambiguously centrosymmetric. (A) without microwave discharge of the gaseous mixture showing the presence of only Cl_2 (for which ^{35}Cl, ^{37}Cl isotope splitting was observed) (B) with microwave discharge of the gaseous mixture, showing the presence of both $XeCl_2$ and Cl_2.

Since our dilute and concentrated spectra appeared essentially the same and our spectral recordings indicate a sensitivity factor of a comfortable 10x to spare for the most dilute runs ($XeCl_2$:Xe = 1:200) and that under such conditions no other Raman lines were observed in the region 60-650 cm^{-1}, the possible presence of $XeCl_4$ could be excluded (by comparison with the spectra of similar square planar isoelectronic species [46, 48]) and $XeCl_2$ favored as the major product of the xenon-chlorine discharge reaction.

An unusual effect was observed when an attempt was made to discover the nature of the decomposition products formed in a diffusion-controlled warm-up study of $XeCl_2$ under conditions of high dilution [43]. A different laser

excitation wavelength produced a resonance phenomenon. Results of this study are shown in Fig. 5 A-D. Spectrum C indicates $XeCl_2$ after discharging a 1:100 mixture of Cl_2:Xe and D shows the same matrix after diffusion at 40K. Both spectra were recorded with the 6471A line of a krypton laser. Analagous spectra were recorded with the 5682A line and these are labelled A and B. The spectra of C and D illustrated the normal diffusion behavior of $XeCl_2$ but, surprisingly, those of A and B indicated an unexpected resonance process. Here the 253 cm^{-1} line of $XeCl_2$ shows an initial increase in intensity after diffusion rather than the expected decrease together with the simultaneous "germination" of new bands at about 470 and 720 cm^{-1}. Although the exact nature and interpretation of these observations are still debatable, the spacing of the bands at approximately 250, 470 and 720 cm^{-1} is roughly the same as that for the first excited electronic state, $^3\Pi_{O^+u}$ of Cl_2 in the gas phase [49], namely 239.4 cm^{-1}. The series of bands may be due to laser-induced resonance fluorescence of excited chlorine produced in the decomposition of $XeCl_2$.

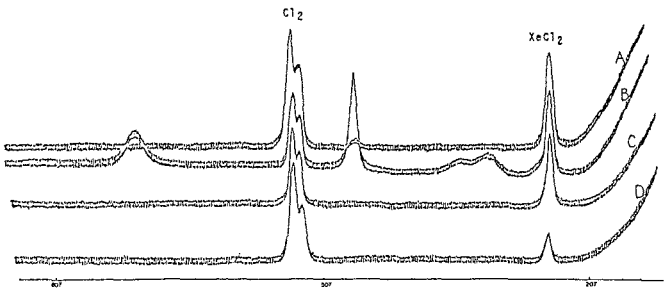

Fig. 5. The Raman spectra of a xenon-chlorine (100:1) matrix at 4.2K after subjecting the gaseous mixture to a microwave discharge. A resonance effect is suspected at approximately 250, 470 and 720 cm^{-1}. (A) 5682A laser excitation (B) 5682A laser excitation after warm up to 40K, (C) the same as (A) but 6471A laser excitation (D) 6471A laser excitation after warm up to 40K.

Matrix Raman Spectrum and Molecular Structure of the Tribromine Radical Br_3

In this section the matrix Raman spectra of the products of Ar/Br_2, Kr/Br_2 and Xe/Br_2 microwave discharges are described. In the experiments a single line was observed at 190, 197 and 196 cm^{-1} for xenon, krypton and argon matrices respectively, apart from the line at about 305 cm^{-1} corresponding to Br_2 [42]. These lines were not present until the gas mixtures were subjected to a microwave discharge.

The data with krypton and xenon as matrix gases (Fig. 6, 7) indicates the formation of the linear tribromine free radical where the single Raman frequency yields a value of 1.70 md/A for the force constant sum $f_r + f_{rr}$. This value when compared with f_r = 2.45 md/A for Br_2 and $f_r + f_{rr}$ = 1.23 md/A for Br_3^- provides evidence that the bonding in linear Br_3 resembles that of the linear Br_3^- tribomide negative ion [50].

The argon matrix yielded the most interesting results(Fig. 8) for the diffusion-controlled warm-up study of Br_3 [43]. Apart from producing the smallest quantities of Br_3 diffusion in argon resulted in new lines. As the matrix was warmed successively to 35, 45 and 55K the 196 cm^{-1} band of Br_3

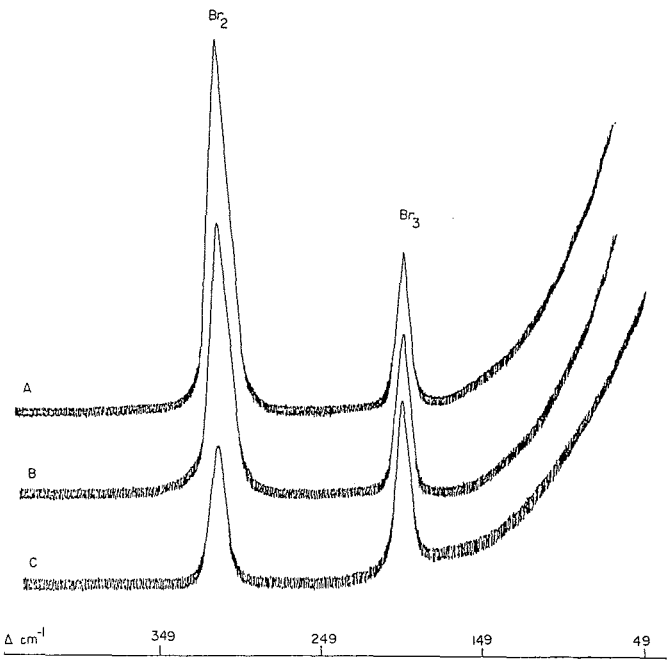

Fig. 6. Through Raman spectroscopy the existence of the free radical Br_3 has been unequivocably proven. The matrix Raman spectrum of the products of a Kr/Br_2 (50:1) microwave discharge (C) frozen at 4.2K, (B) and (A) allowed to diffuse at 35K for 3 and 6 minutes respectively and then recooled to 4.2K. As the matrix is allowed to warm up the reactive Br_3 reverts to Br_2.

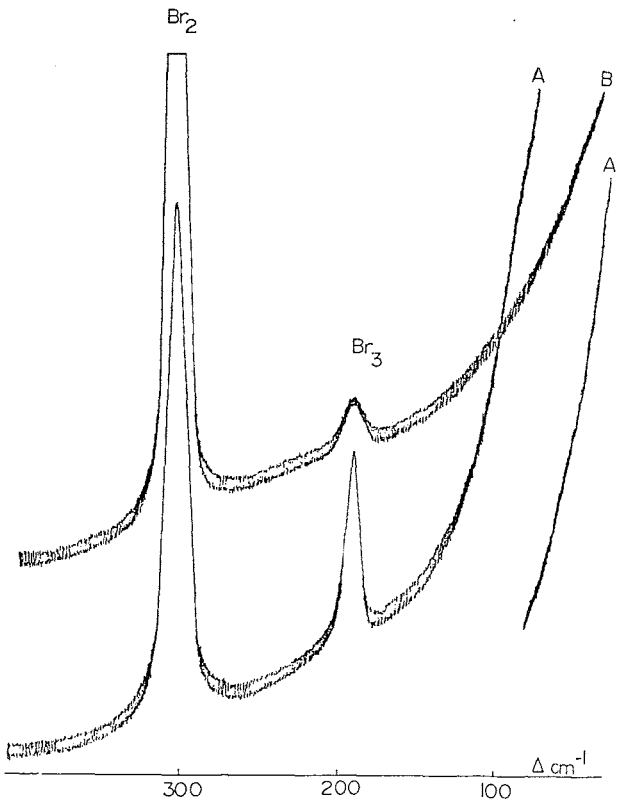

Fig. 7. To prove the existence of Br_3 the experiment was repeated in Xe and Ar matrices. The matrix Raman spectrum of the products of a Xe/Br_2 (50:1) microwave discharge (A) frozen at 4.2K, (B) allowed to diffuse at 35K for 3 minutes and then recooled at 4.2K.

gradually disappeared to be replaced by new bands at 179 cm^{-1} and 214 cm^{-1}. These lines are undoubtedly bromine-bromine strectching modes, compatible with either a T-shaped Br_4 or a square planar Br_5 molecule formed by diffusion and reaction of the various species (Br, Br_2 or Br_3) in the argon matrix. The data, however, is not sufficiently definitive to allow a clear- cut distinction between the two structures.

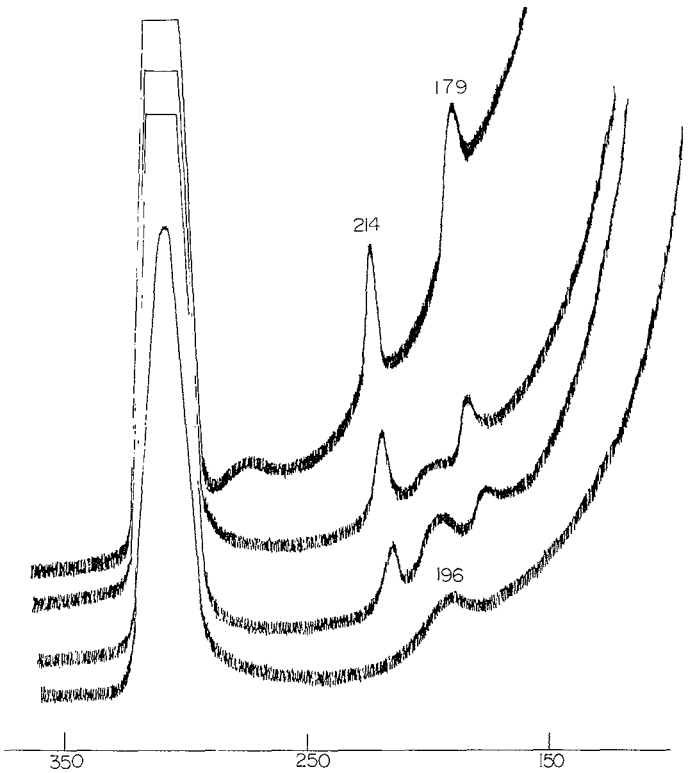

Fig. 8. The matrix Raman spectra of the products of an Ar/Br_2 (50:1) microwave discharge (A) frozen at 4.2K, (B), (C) and (D) after successive diffusion controlled warm up experiments at 35K.

The Matrix Raman Spectra of High Temperature Species

Selenium Dioxide Monomer and Dimer

Selenium dioxide normally exists as an oxygen-bridged chain polymer (A) in the solid state and a non-linear tri-atomic molecule (B) in the vapor phase (approximately 99% monomeric) [51-56].

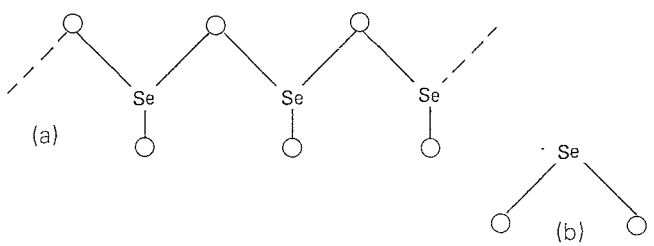

The matrix Raman spectra [57] of monomeric SeO_2 are, as expected, very similar to the corresponding gas-phase Raman spectra apart from small matrix shifts. However, diffusion of SeO_2 monomer in the matrix in a controlled warm-up study showed many stages in the polymerization process. Bands could be associated with the first stage of the polymerization process and assigned to $(SeO_2)_2$. The Raman data for $(SeO_2)_2$ together with normal co-ordinate calculations for various possible structures of $(SeO_2)_2$ indicated that the C_{2h} *trans* form (with a double oxygen bridge) was favored for the dimer C.

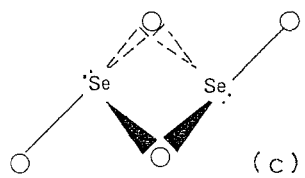

Germanium Difluoride Monomer and Dimer

In the only reported matrix infrared study [58] of monomeric GeF_2 produced by vaporizing solid (polymeric) GeF_2, the spectra were always complicated by the presence of higher aggregates in the matrix. This was unavoidable and not necessarily the result of poor isolation (mass spectroscopic data [59] for the vapor above solid GeF_2 have shown the presence of $(GeF_2)_n$ where n = 1, 2, 3 and 4).

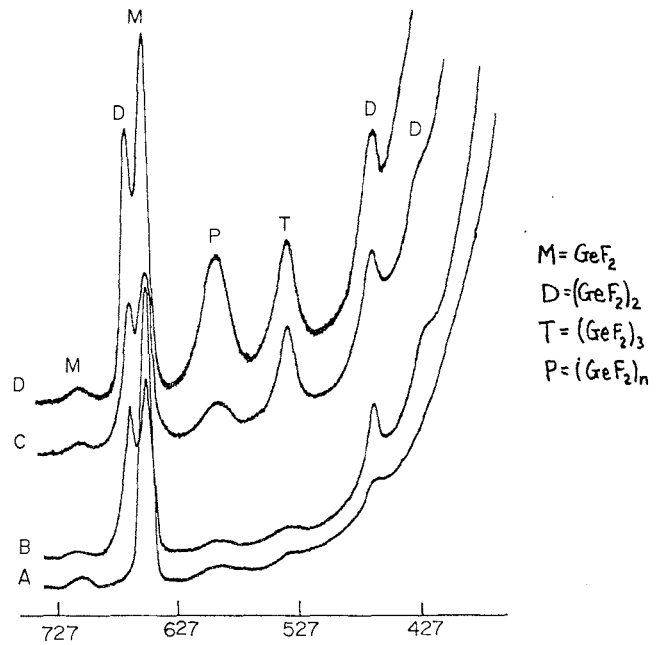

Fig. 9. Spectroscopically pure, monomeric GeF_2 was produced in a gas flow, high temperature Knudsen cell by the reaction of GeF_4 with Ge. As the matrix isolated monomer warmed up to 35K (Spectra A-D) features representing dimer (D), trimer (T) and possibly polymer (P) appear.

We were particularly interested in $(GeF_2)_2$ as it was likely to have the same molecular configuration as $(SeO_2)_2$. The gas-flow Knudsen cell reaction technique [45] proved to be an efficient way of producing almost pure GeF_2 monomer (Fig. 9) by the reaction.

$$GeF_4 + Ge + N_2 \xrightarrow[\text{Knudsen cell}\ 300C]{\text{gas flow}\ \text{stainless steel}} GeF_2$$

The monomer spectrum of GeF_2 in a nitrogen matrix [45] was definitive for ν_1 and ν_3. Polarization data on the matrix identified ν_1 ($\rho_p \cong 0.55$).

By recording spectra after successive diffusion controlled warm-up experiments the progress and results of the polymerization process of GeF_2 monomer in the matrix were observed (Fig. 9). Best results were obtained in a N_2 matrix and three lines could be associated with $(GeF_2)_2$ and most satisfactorily assigned to a double fluorine-bridged, non-planar structure (Table 1) rather than a structure containing a Ge-Ge bond. $(SiF_2)_2$ is thought to contain a Si-Si bond [45].

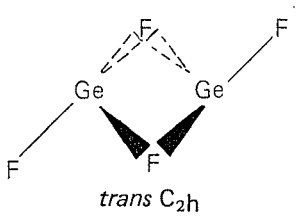

trans C_{2h}

Table 1

Observed* and Calculated Raman Frequencies for Germanium Difluoride Dimer $(GeF_2)_2$

Observed (N_2 Matrix)**	Calculated	Assignment C_{2h} and Approximate Descriptions
669 s	663	$a_g\nu GeF_t$
465 ms	473	$a_g\nu GeF_b$
424 w	436	$b_g\nu GeF_b$
	241	$a_g\delta GeF_t$
	204	$b_g\delta GeF_b$
	137	$a_g\nu GeGe$

* GeF_2 monomer bands observed at 702 w and 653 s in a N_2 matrix and $(GeF_2)_3$ trimer observed at 533 cm^{-1}.

** Scans covered the range 270-1000 cm^{-1} in the N_2 matrix.

Monomeric Tin and Lead Dichlorides and Dibromides

Electron diffraction [64] data has shown the existence of non-linear triatomic MX_2 molecules as the major vapor species in the gas phase for M = Sn or Pb and X = Cl or Br. Recording of high-temperature gas-phase spectra of these species has often been rendered impossible by laser-induced resonance fluorescence processes and decomposition [60 - 63].

The matrix Raman spectra for tin and lead dichlorides [14, 66] and dibromides unequivocably demonstrate the suitability of the technique for obtaining not only data complementary to infrared work [65] but also for studying otherwise spectroscopically inaccessible species. Results indicate also that spectral sensitivities and resolution can be achieved which are comparable with the complementary infrared data [65] (see the ^{35}Cl and ^{37}Cl isotope splitting for ν_1 and ν_3 of monomeric $PbCl_2$) and that matrix Raman polarization measurements can add a valuable new tool for matrix isolation studies (see the identification of ν_1 and ν_3 for $PbCl_2$, $PbBr_2$ and $SnBr_2$).

The observation of two Raman active metal-halogen stretching modes, provides evidence of the non-linear geometry of the MX_2 monomers (Fig. 10 - 12).

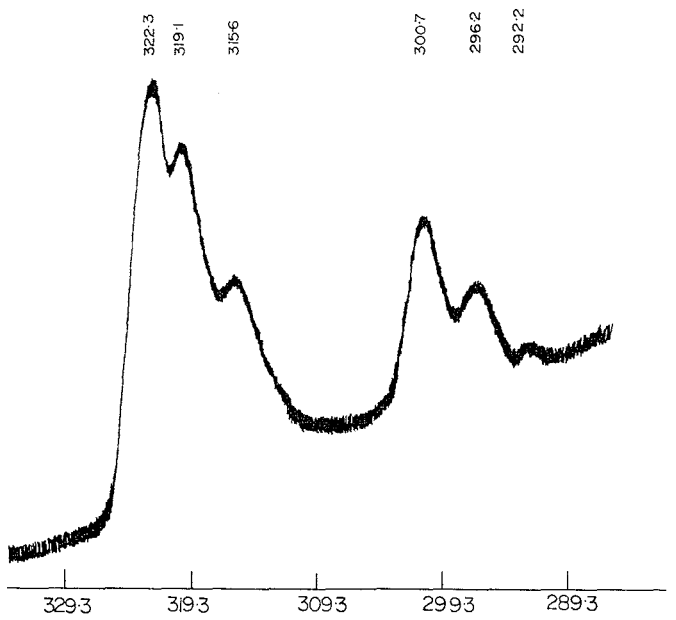

Fig. 10. The matrix Raman spectrum of monomeric $PbCl_2$ in argon (M/A ≅ 300) under high resolution (spectral slit 1 cm^{-1}) showing the ^{35}Cl, ^{37}Cl isotope components of ν_1 and ν_3 arising from symmetric and antisymmetric Pb-Cl stretching modes of $Pb^{35}Cl_2$, $Pb^{35}Cl^{37}Cl$ and $Pb^{37}Cl_2$ respectively. All three possible combinations of chlorine isotope components appear and their relative intensities correspond to their relative natural abundance.

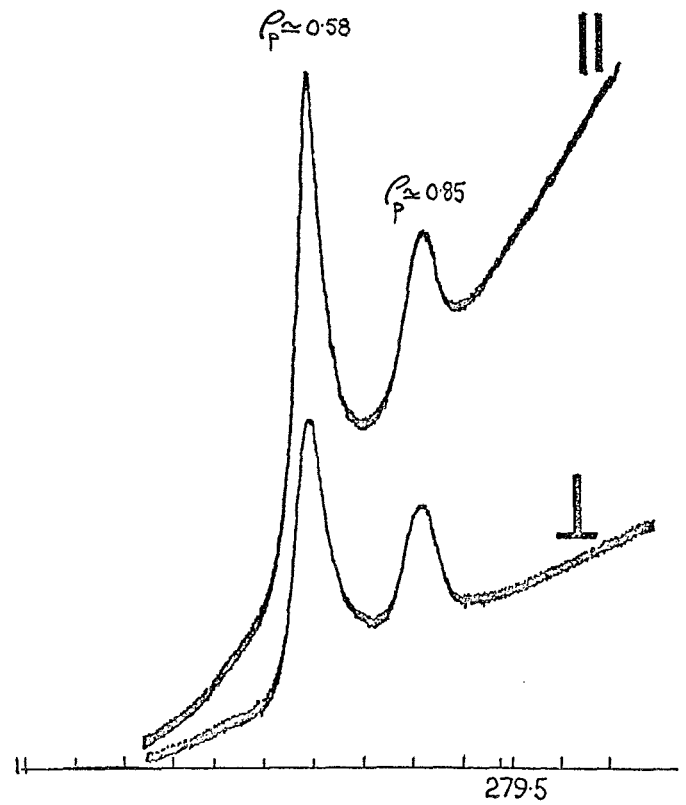

Fig. 11. For the first time depolarization measurements have been made on highly reactive matrix isolated species. Spectra of $PbCl_2$ in N_2 showing parallel and crossed polarizations are presented.

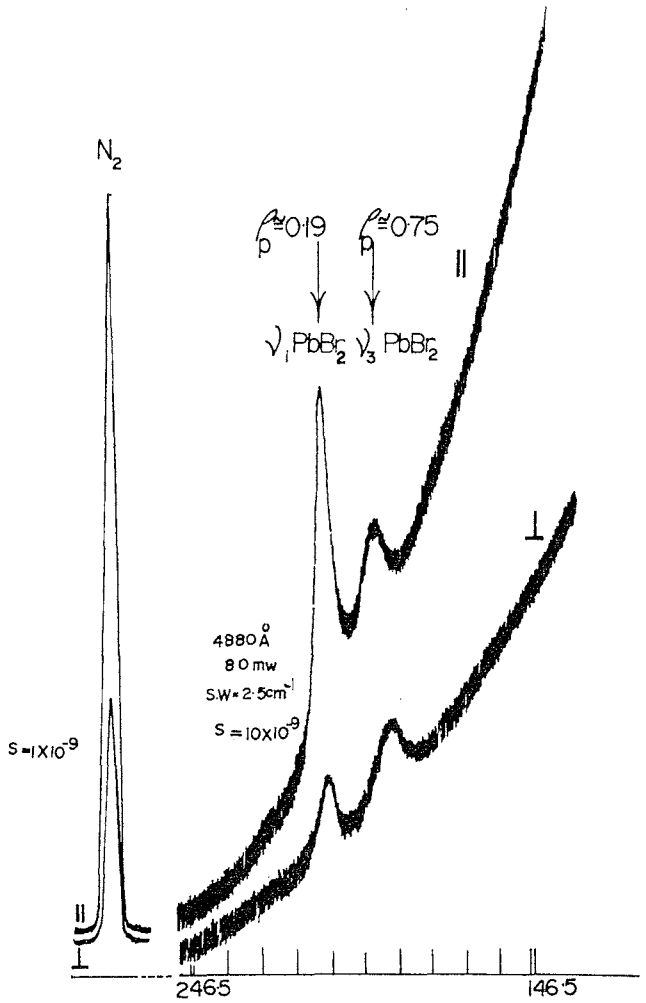

Fig. 12. Depolarization measurements have been found to be feasible down to 150 cm^{-1} as depicted with monomeric $PbBr_2$. Attempts to do this in the gas phase have often proved impossible because at high temperatures resonance effects and decomposition occur.

Matrix Raman Spectrum and Bonding in the Lithium Superoxide Molecule LiO_2

Using a lithium atom-oxygen co-condensation reaction, we have obtained the first Raman data for matrix-isolated LiO_2 and Li_2O_2 (Fig. 13). The Raman data for LiO_2 was particularly helpful for testing the proposed structure [70, 71] and bonding in LiO_2. This was confirmed to be electrostatic in nature, consisting of a Li^+ cation interacting with an O_2^- anion as a C_{2v} ion pair [68, 72].

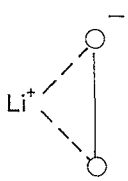

In the presence of higher concentrations of lithium the matrix isolated Li_2O_2 species was formed [68] and showed only the strong Raman active νO-O stretching mode at 802 cm^{-1} of the O_2^{2-} anion, which is expected for a species bonded similarly to that of LiO_2 (Fig. 13C).

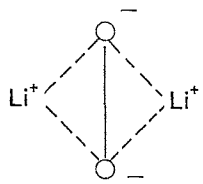

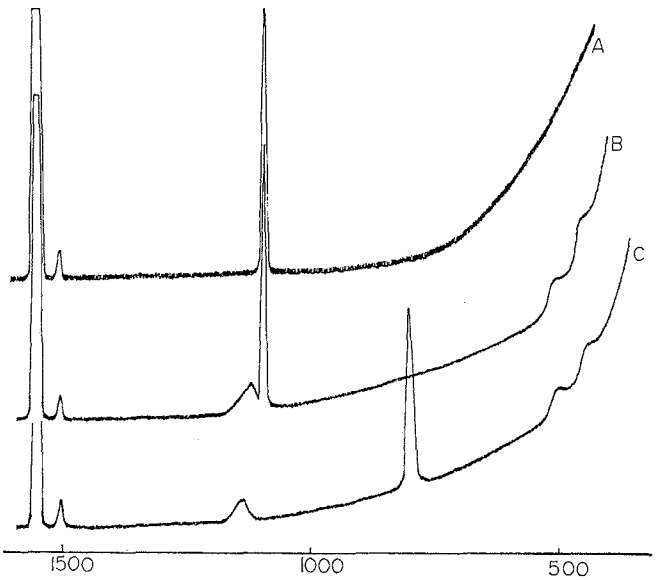

Fig. 13. Because only one strong line appears in A and B at 1097 cm^{-1} the hypothesis of Andrews [70] obtained from the corresponding infrared data, that the bonding in LiO_2 is electrostatic, is confirmed. The transformation of LiO_2 to Li_2O_2 is shown in C on warming the matrix shown in B.

Matrix Raman Spectrum of the Dichlorophosphinyl Radical PCl_2 in Solid Argon; Evidence for Diatomic Lithium Li_2 in Solid Argon

Phosphinyl radicals are of considerable interest as possible intermediates in a variety of chemical reactions [73]. Andrews first reacted lithium with PCl_3 in argon [74] to obtain matrix infrared evidence for the free radical PCl_2. Although IR absorption intensities were very weak relative to the precursor PCl_3, he observed two PCl stretching modes at approximately 523 and 449 cm^{-1} and ascribed them to the non-linear, triatomic free radical PCl_2. Because these bands were of comparable intensity, however, their assignment to ν_1 and ν_3 was not obvious.

Raman measurements permitted a definitive assignment. Working with matrix-to-solute ratios similiar to those recommended by Andrews (Li:PCl_3:Ar = 1:1:200), we co-condensed an atomic beam of lithium with PCl_3 in argon (Fig. 14). Apart from the bands due to lithium chloride monomer and dimer (N) and PCl_3 (R) a line is observed at approximately 527 cm^{-1} (P) almost coincident with the reported infrared band at 525-523 cm^{-1}. This defines ν_1 of PCl_2 as the higher of the two observed stretching modes. A much weaker band at approximately 450 cm^{-1} (P) is probably ν_3, coincident with the infrared band at 452-447 cm^{-1}. Since both lines completely disappeared in a diffusion-controlled warm-up at 30K, the formation and identity of PCl_2 and the assignment of ν_1 and ν_3 are confirmed.

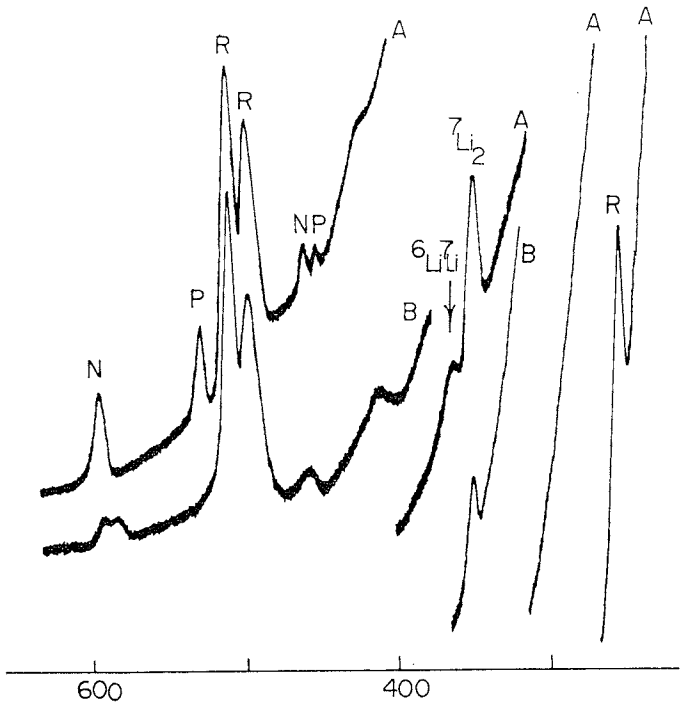

Fig. 14. The existence of the free radical PCl_2 which was first observed by Andrews in the infrared is unambiguously assigned by the matrix Raman spectrum at (P). In this warm-up reaction from Spectrum A to B Li atoms produced the free radical species by the reaction $PCl_3 + Li \rightarrow PCl_2 + LiCl$. The Raman spectrum of the diatomics $^7Li_2$ and $^7Li^6Li$ in natural abundance appeared too.

An advantage of the matrix Raman technique in this type of study is that lines arising from homonuclear diatomics may be observed and identified, whereas they are inactive in the infrared. The question as to whether Li_2 is formed in the matrix during deposition is clearly answered by the PCl_2 matrix Raman spectrum which shows two lines at 352 and 365 cm^{-1} whose frequencies, isotopic shifts and intensities are those expected for the isotopic molecules $^7Li_2$ and $^6Li^7Li$ respectively [75] present in natural abundance. The formation of products in the Li/O_2 co-condensations (other than LiO_2 and LiO_2Li) from the reaction of Li_2 with O_2 is probably quite reasonable [70].

AN approximation, termed the "cold gas model", considers the guest species to be an infinitely dilute cold gas where the host species is assumed absent [19]. Thus all intramolecular processes are assumed to occur without environmental influence. The cold gas model may be applied to matrix Raman spectra where the guests are assumed to be a perfectly random collection of non-interacting species in a weakly interacting host.

In this treatment of Raman depolarization measurements on matrix isolated species, the isotropic optical behavior of a transparent medium (for example, the fcc lattice of the inert gases and N_2) facilitates the observations. Provided the matrix support is transparent, depolarization of the incident laser beam and the scattered Raman light should be minimal and experimental depolarization ratios should be meaningful for matrix-isolated species. Although perfectly transparent matrices are difficult to obtain in practice and non-ideal depolarization ratios will inevitably result from frosty matrices, the data permits symmetry assignments.

Referencing the classical expressions for randomly oriented molecules in a matrix (or fluid), we are not surprised to find that for ideal Raman scattering from matrices, the same equations apply as for fluids where a band may be assigned to a totally symmetrical mode if its depolarization ratio is less than ¾.

Raman depolarization measurements have already been realized in practice for both stable and unstable matrix isolated species [13, 14]. Nibbler [13] reported depolarization measurements of various stable molecules such as, CCl_4, CH_4, CO_2, CS_2, COS in N_2 matrices (at $M/A \cong 500$). Although the measured depolarization ratios were not ideal they were sufficiently clear cut to distinguish totally symmetrical from depolarized asymmetrical modes. Other examples which demonstrate the usefulness of these measurements are the unstable monomeric dihalides of group IV [14].

AS with any new technique in its early stages of development, matrix Raman spectroscopy is certainly amenable to refinement:

1. Increasing signal-to-noise and throughput

   (a) silvered, rather than aluminized optics for higher reflectivity
   (b) finer ruled gratings to permit wider slits without sacrificing bandpass
   (c) improved illumination - collection optics to gather more light
   (d) dye lasers and the possible utilization of resonance conditions.

2. Optimizing detection

   Improved, high quantum efficiency photomultiplier tubes, for example, the RCA developmental C-31034.

3. Closer approach to the excitation line

   (a) a 3rd monochromator
   (b) a single moded laser with iodine filter

Matrix isolation Raman spectroscopy is almost certain to develop rapidly in the years ahead as practical applications of this powerful technique for studying reaction mechanisms and intermediate species are discovered.

ACKNOWLEDGEMENTS

I am sincerely grateful to Mr. David Boal, Mr. Helmhut Huber, Mr. Anthony Vander Voet, Mr. Dennis Frieson and Dr. Martin Moskovits for their technical assistance, many helpful discussions, enthusiasm and patience which they have given toward the development of the various aspects of matrix isolation laser Raman spectroscopy at the University of Toronto. I would like to thank Professor A.G. Brook and Professor E.A. Robinson for their continued encouragement of our work and the National Research Council of Canada and Research Foundation for financial support.

REFERENCES

1. a) A. Cabana, A. Anderson and R. Savoie, J. Chem. Phys., 1965, **42**, 1122.
   b) E. Nixon, Raman Newsletter, 1969.
   c) I.R. Beattie and R. Collis, J. Chem. Soc. (A), 1969, 2960.
   d) P.A. Giguere, K. Herman and X. Deglise, Paper J11, Abstracts of the 25th Symposium on Molecular Structure and Spectroscopy, The Ohio State University, 1970.
   e) D. O'Hare and G. Leroi, 2nd International Raman Spectroscopy Conference, Oxford University, 1970.
   f) H.H. Claassen and J. Shirk, J. Chem. Phys., 1971 (in press).
   g) H.H. Claassen and J.L. Huston, J. Chem. Phys., 1971, **55**, 1505.
2. J. Dewar, Proc. Roy. Soc. 1901, **68**, 360.
3. L. Vergard, Nature, 1924, **113**, 716.
4. G.N. Lewis and D. Lipkin, J. Amer. Chem. Soc., 1942, **64**, 2801.
5. M. Freamo and F.O. Rice, J. Amer. Chem. Soc., 1951, **73**, 5529.
6. A.M. Bass and H.P. Broida, 'Formation and Trapping of Free Radicals', 1960, Academic Press, New York and London (and references therein).
7. I. Norman and G. Porter, Nature, 1954, **174**, 508.
8. E. Whittle, D.A. Dows and G.C. Pimentel, J. Chem. Phys., 1954, **22**, 1943.
9. G.C. Pimentel, G.E. Ewing and W.E. Thompson, J. Chem. Phys., 1960, **32**, 927.
10. E.D. Becker and G.C. Pimentel, J. Chem. Phys., 1956, **25**, 224.
11. M.J. Linevsky, J. Chem. Phys., 1961, **34**, 587.
12. W. Weltner, Proc. Int. Symp. Condensation and Evaporation of Solids, 1962, 243.
13. J. Nibbler and D. Coe, J. Chem. Phys., **55**, 5133.
14. H. Huber, G.A. Ozin and A. Vander Voet, Nature, 1971, **232**, 166.
15. A. Snelson, J. Phys. Chem., 1967, **71**, 3202.
16. E.J. Ambrose, A. Elliot and B.R. Temple, Proc. Roy. Soc. Lond., A, 1951, **206**, 192. G.C. Pimentel and A.J. McLellan, J. Chem. Phys., 1952, **20**, 270.
17. W.G. Fately, H.A. Bent and B. Crawford, J. Chem. Phys., 1959, **31**, 204.
18. M.M. Rochkind, Science, N.Y., 1968, **160**, 197.
19. B. Meyer, "Low Temperature Spectroscopy", Elsevier, New York, 1971.
20. E.D. Becker, G.C. Pimentel and M. Van Thiel, J. Chem. Phys., 1957, **26**, 145. G.C. Pimentel, S.W. Charles and Kj. Rosengren, J. Chem. Phys., 1966, **44**, 3029.
21. A. Snelson, J. Chem. Phys., 1967, **46**, 3652.
22. W. Weltner and J.R.W. Warn, J. Chem. Phys., 1962, **37**, 292.
23. W. Weltner, P.N. Walsh and C.L. Angell, J. Chem. Phys., 1964, **40**, 1299.
24. S.J. Cyvin, B.N. Cyvin and A. Snelson, J. Phys. Chem., 1971, **75**, 2609.
25. A. Snelson, J. Phys. Chem., 1970, **74**, 537.
26. L. Andrews, J. Chem. Phys., 1968, **48**, 972.
27. L. Andrews and G.C. Pimentel, J. Chem. Phys., 1966, **44**, 2361.
28. L. Andrews, J. Chem. Phys., 1971, **54**, 4935.
29. H. Huber, G.A. Ozin and A. Vander Voet (unpublished work).
30. M.E. Jacox and D.E. Milligan, J. Chem. Phys., (in press).
31. V. Bondybey, G.C. Pimentel and P.N. Noble, J. Chem. Phys., 1971, **55**, 540.
32. L.Y. Nelson and G. Pimentel, J. Chem. Phys., 1967, **47**, 3671.
33. A. Arkell, R.R. Reinhard and L.P. Larson, J. Amer. Chem. Soc., 1965, **87**, 1016.
34. M.E. Jacox and D.E. Milligan, J. Chem. Phys., 1964, **40**, 2461. M.E. Jacox and D.E. Milligan, J. Chem. Phys., 1964, **41**, 2838.
35. A.J. Rest and J.J. Turner, Chem. Comm., 1969, 1026.
36. N.G. Moll, D.R. Clutter and W.E. Thompson, J. Chem. Phys., 1966, **45**, 4469.
37. J.J. Turner and G.C. Pimentel in "Noble Gas Compounds", University of Chicago Press, 1963.
38. G.C. Pimentel, R.D. Spratley and J.J. Turner, J. Chem. Phys., 1966, **44**, 2063.
39. M.E. Jacox and D.E. Milligan, J. Chem. Phys., 1971.
40. P.N. Noble and G.C. Pimentel, J. Chem. Phys., 1968, **49**, 3165.
41. L.Y. Nelson and G. Pimentel, Inorg. Chem., 1967, **6**, 1758.
42. D. Boal and G.A. Ozin, J. Chem. Phys., 1971, (in press).
43. D. Boal and G.A. Ozin (unpublished results).
44. D. Boal and G.A. Ozin, Spectroscopy Letters, 1971, **4**, 43.
45. G.A. Ozin and A. Vander Voet (unpublished results).
46. J.D.S. Goulden, A. Maccoll and D.J. Millen, J. Chem. Soc., 1950, 1635.
47. H. Meinert, Z. Chem., 1966, **6**, 71.
48. H. Stammereich and R. Forneris, Spectrochim. Acta, 1960, **16**, 363.
49. R.S. Mulliken, Physics Rev., 1940, **57**, 500.
50. W.B. Person, A.R. Anderson, J.N. Fordemwalt, H. Stamreich, and R. Forneris, J. Chem. Phys., 1961, **35**, 908.
51. J.D. McCullough, J. Amer. Chem. Soc., 1937, **59**, 789.
52. K.J. Palmer and W. Elliot, J. Amer. Chem. Soc., 1938, **60**, 1852.
53. P.A. Giguere and M. Falk, Spectrochim. Acta, 1960, **16**, 1.
54. I.R. Beattie and J. Horder, (private communication).
55. J.W. Hastie, R. Hauge and J.L. Margrave, J. Inorg. Nucl. Chem., 1969, **31**, 281.
56. P.J. Ficarlora, J.L. Margrave, J.C. Thompson, J. Inorg. Nucl. Chem., 1969, **31**, 3771.
57. D. Boal, G. Briggs, H. Huber, G.A. Ozin, E.A. Robinson, and A. Vander Voet, Nature, 1971, **231**, 174.
58. J.W. Hastie, R. Hauges and J.L. Margrave, J. Phys. Chem., 1968, **72**, 4492.
59. K.F. Zmbov, J.W. Hastie, R. Hauge and J.L. Margrave, Inorg. Chem., 1968, **7**, 608.
60. I.R. Beattie, G.A. Ozin and R.O. Perry, J. Chem. Soc., A, 1969, 2071.
61. G.A. Ozin, Chem. Comm., 1969, 1325.
62. I.R. Beattie and R.O. Perry, J. Chem. Soc., A, 1970, 2429.
63. G.A. Ozin, Progress Inorg. Chem., 1971, **14**, 173.
64. M.W. Lister and L.E. Sutton, Trans. Faraday Soc., 1941.
65. L. Andrews and D.L. Frederick, J. Amer. Chem. Soc., 1970, **92**, 775.
66. H. Huber, G.A. Ozin and A. Vander Voet, Nature, 1971, 232, 166 and J. Molecular Spectroscopy, 1971, (in press).
67. L. Andrews and G.C. Pimentel, J. Chem. Phys., 1961, **44**, 2361.
68. H. Huber and G.A. Ozin, J. Mol. Spectroscopy (in press).
69. H. Huber and G.A. Ozin (unpublished work).
70. L. Andrews, J. Chem. Phys., 1969, **50**, 4288.
71. J. Rolfe, W. Holzer, W.F. Murphy, and H.J. Bernstein, J. Chem. Phys., 1968, **49**, 963.
72. J.H.B. George, J.A. Rolfe, L.A. Woodwood, Trans. Faraday Soc., 1953, **49**, 375.
73. D.E.C. Corbridge, M.S. Pearson and C. Walling, "Topics in Phosphorus Chemistry", Vol. 3, Interscience Publishers, New York, N.Y. 1966.
74. L. Andrews and D.L. Frederick, J. Phys. Chem., 1969, **73**, 2774.
75. G. Herzberg "Diatomic Molecules", D. Van Nostrand Co. Inc., New York, 1964.
76. H. Huber, P. Kundig, M. Moskovits and G.A. Ozin, Nature Physical Science, 1971, (in press).

No. 1442

THE THIRD MONOCHROMATOR

In Raman spectra of powders and other opaque samples, the Rayleigh and Tyndall scatter frequently shroud lines fundamental to complete low frequency analyses. THE THIRD MONOCHROMATOR serves to reduce the scattered light as demonstrated in the attached Spectra of powdered Boric acid. Spectrum A was recorded on a Spex double monochromator with 2 cm^{-1} spectral slits and about 100 mW of laser power. With THE THIRD MONOCHROMATOR and otherwise identical conditions, the scattered light rejection is significantly improved to reveal two additional Raman lines between 30 and 50 cm^{-1}.

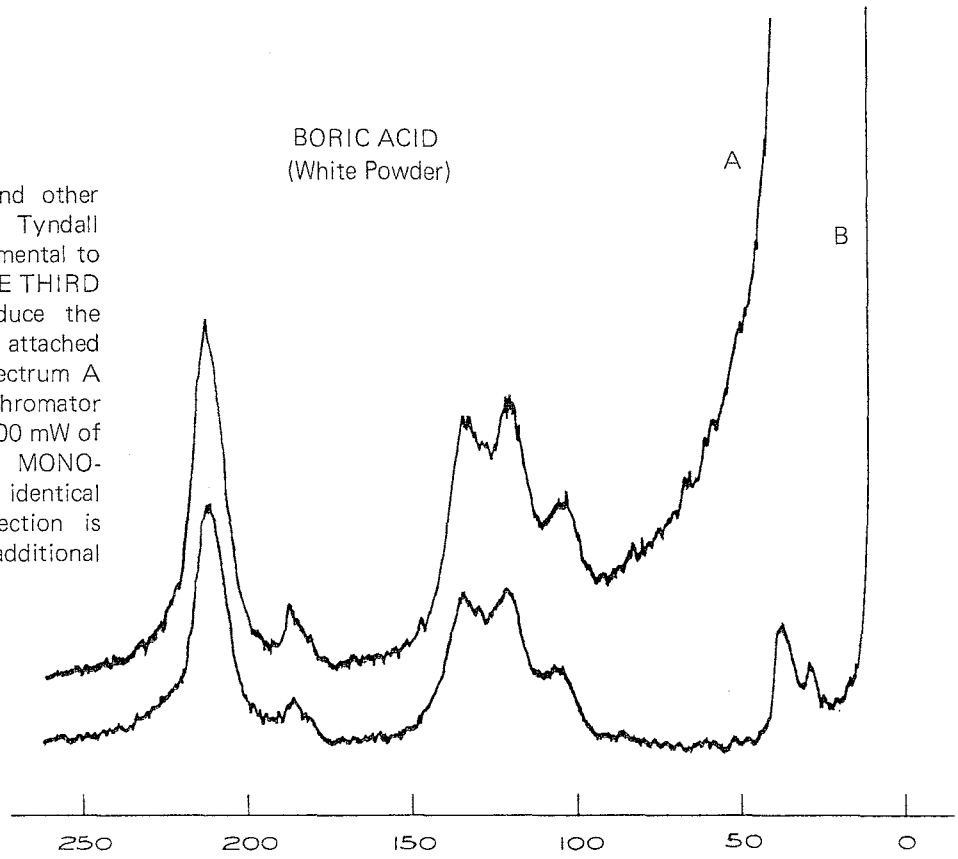

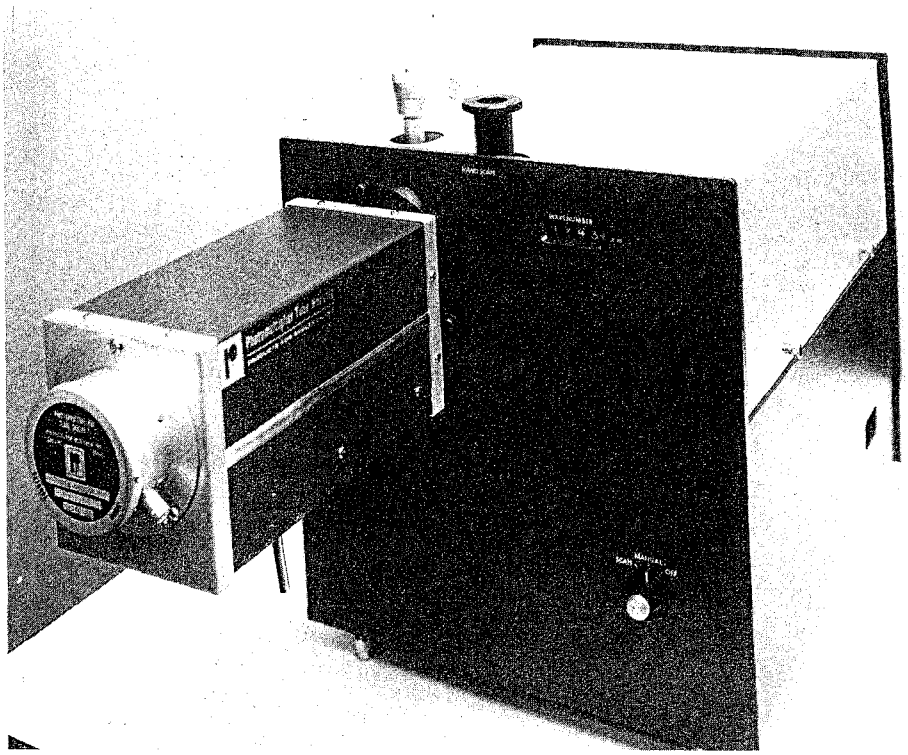

Fig. 1

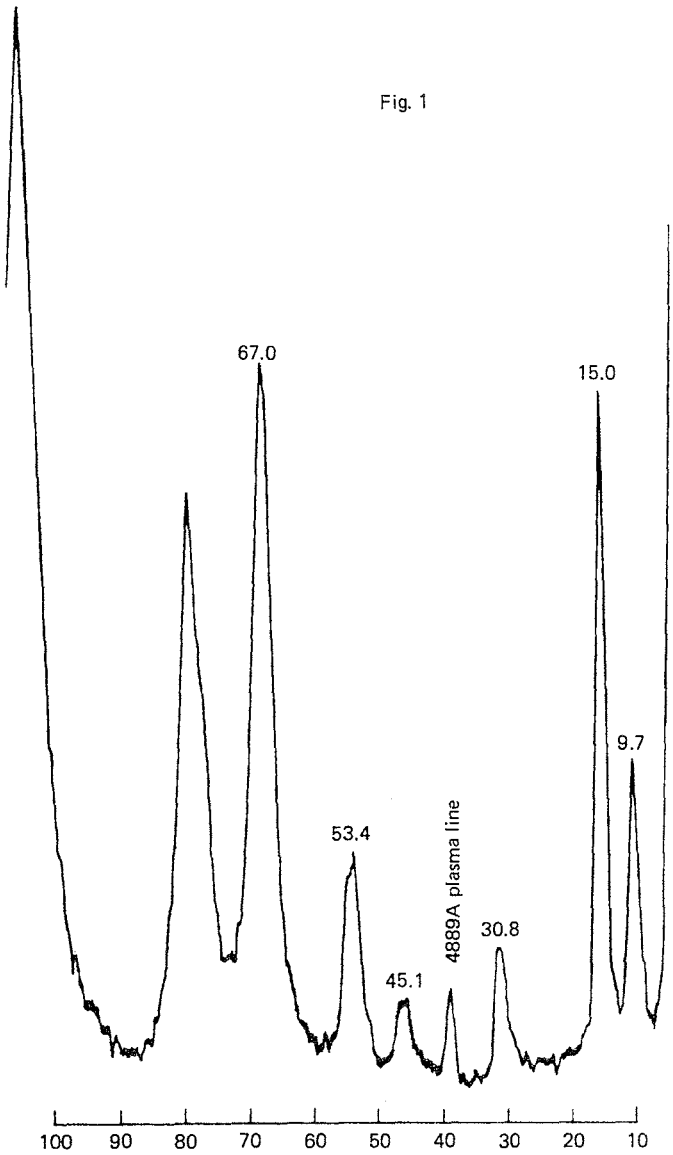

THE THIRD MONOCHROMATOR provides the versatility of a triple monochromator as an accessory to the more widely applicable 1401 Double Monochromator. You need not pay for it either in price or lessened throughput unless you need its features. The 1442 is basically a high-dispersion grating instrument interspersed between the exit slit of the double monochromator and the photomultiplier. Slaved to the scanning drive of the Double the Third tracks along obediently. It acts as a square-wave, bandpass filter, occulting the laser line and its associated grating ghosts. In so doing, Raman lines very close to the exciting line are brought out; the most dramatic example thus far being the 9.7 cm^{-1} line of l-cystine (Fig. 1). Further from the exciting line THE THIRD MONOCHROMATOR reduces the intensity of scattered light including ghosts by a factor of at least 10^{4}.

Whether coupled to an old or New Spex Double Spectrometer, THE THIRD MONOCHROMATOR includes still another feature. For samples that do not require the additional filtering, the grating in the 1442 can be flipped out of the path and a high-reflectance dielectric mirror is substituted. The loss in optical speed is thereby negligible, an important consideration when running weakly scattered materials such as gases and many liquids.

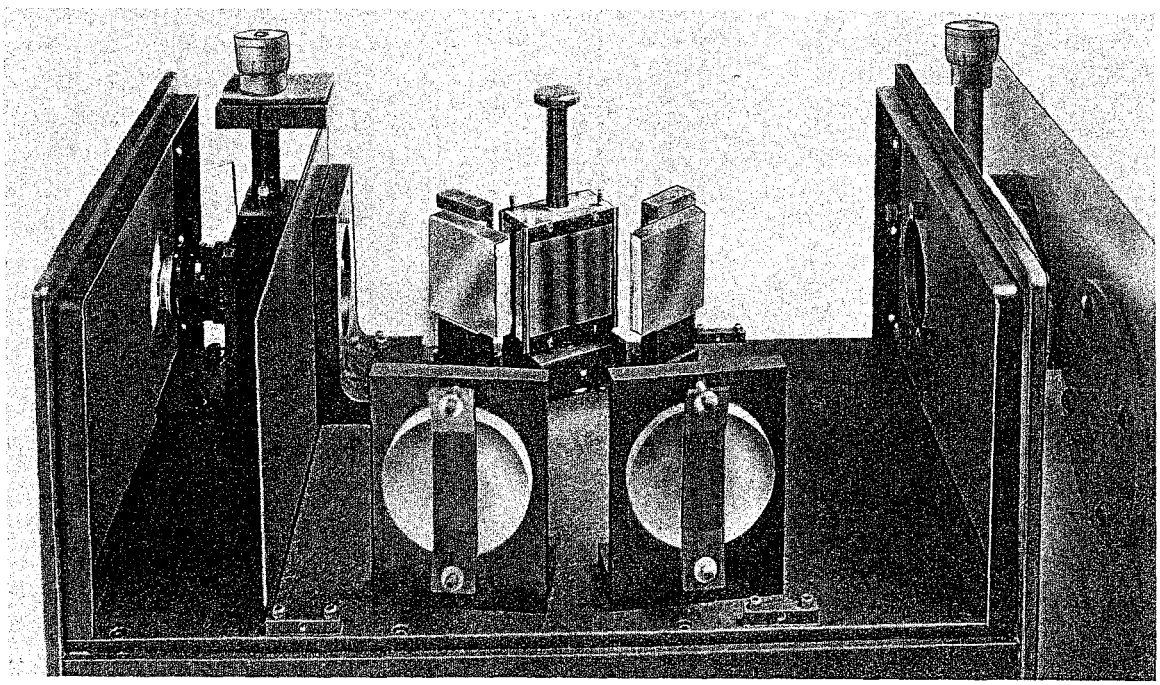

Raman Illuminator No. 1419A

This is an assembly of optics for focussing a laser beam on a gas, liquid or solid sample to provide a diffraction limited spot on the optical axis of the spectrometer. Included are all optics for the analysis of liquids and powders, a 2 ml liquid cell with holder and 100 capillaries with holder. Additional kinematic holders are readily interchangeable for liquids as diminutive as 0.1μl or as large as several ml, powders, pressed discs, single crystals or solid chunks.

The open-ended sample compartment accommodates dewars or furnaces of all types. Collection optics are in a closed individual compartment attached to the entrance slit so they are unaffected by room lighting during sample changes or at times when the sample section is open-ended to accommodate bulky equipment. Polarization rotators, neutral density and interference filters may be permanently mounted.

Once aligned, the laser excitation beam remains fixed in relation to the slit, greatly facilitating alignment of a sample. To compensate for small irregularities in capillaries, differences in refractive index of samples, etc., calibrated controls are provided for moving the sample and focusing the scattered radiation on the entrance slit.

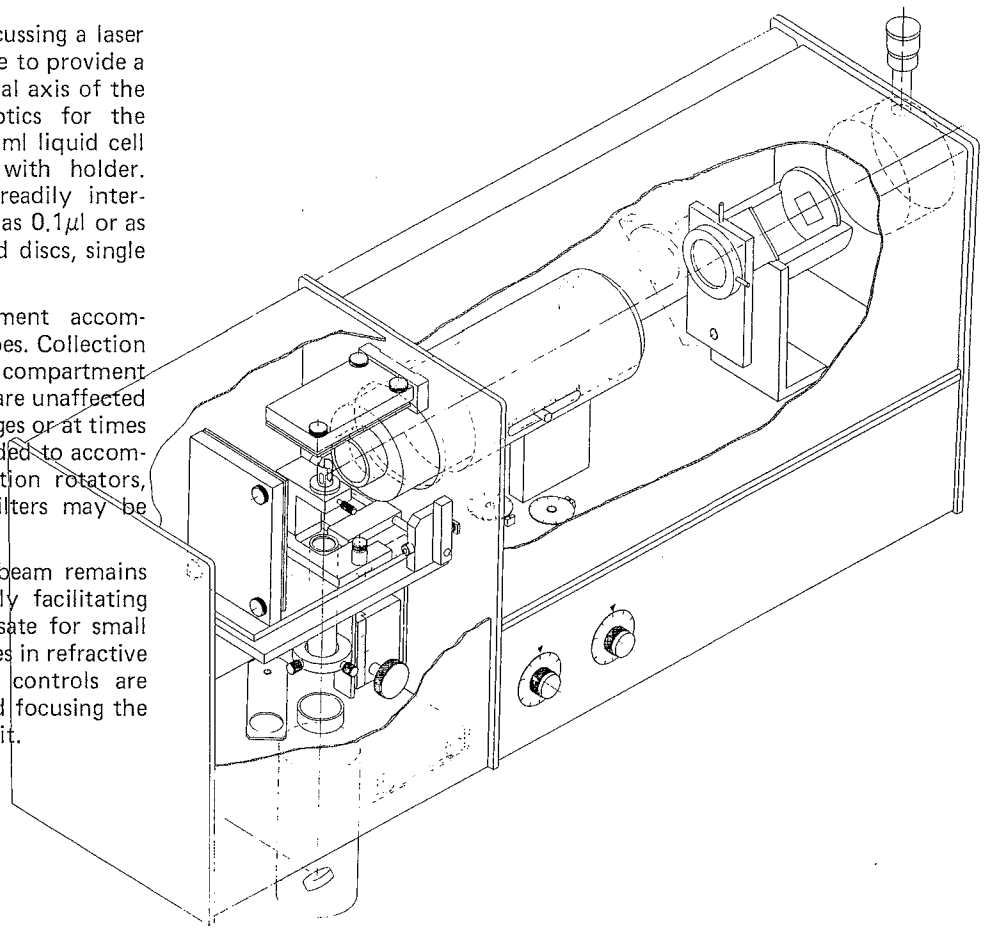

1443A EXTERNAL RESONATING CAVITY

This accessory provides for convenient multipassing of a gas, increasing Raman scatter at least an order of magnitude over a single pass. With just 500 mW of laser power the signal is sufficient to briskly record a 0.7 cm^{-1} splitting in the rotational spectrum of air, as shown. The scanning speed here was 5 cm^{-1}/min; spectral resolution was 0.5 cm^{-1}. It is noteworthy that resolution of this order is readily achievable with photoelectrically recorded Raman spectra on a RAMALOG 4.

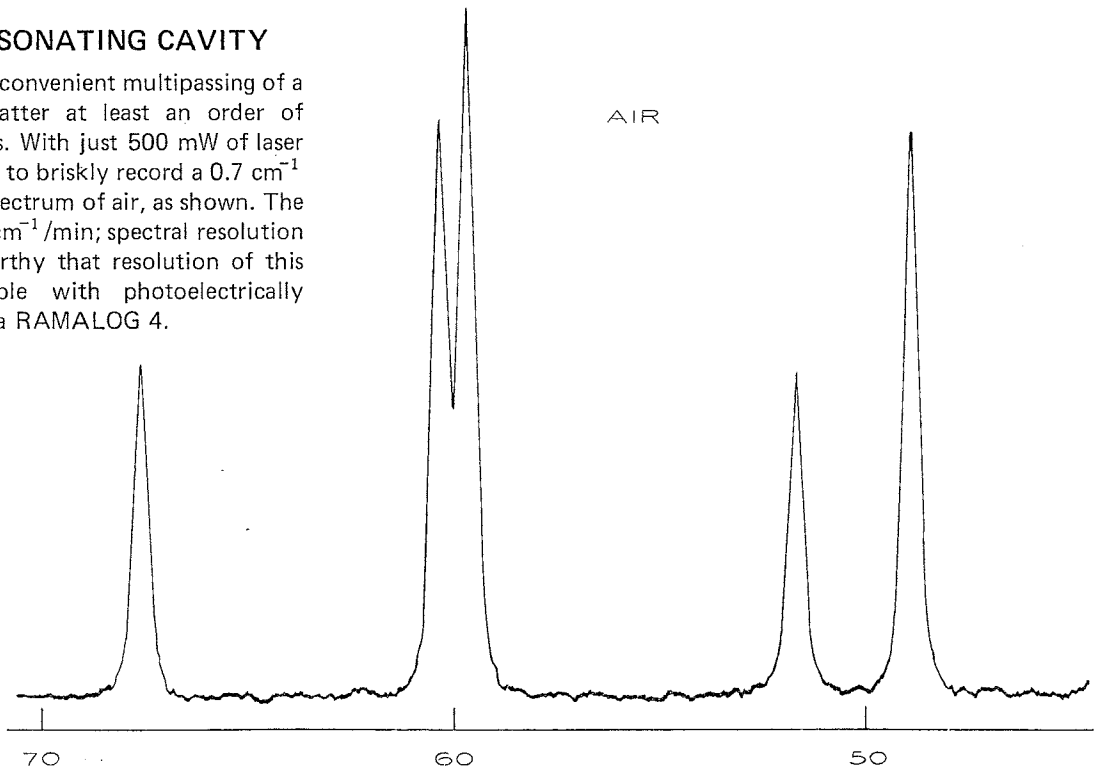

1401 Double Spectrometer

CURRENT ABBREVIATED SPECIFICATIONS

FOCAL LENGTH:	0.85 meter*
SPECTRAL COVERAGE:	31000 cm^{-1} to 10000 cm^{-1} (3225A to 10000A)
APERTURE:	f/7.8
SPECTRAL PURITY:	with monochromatic source, $<10^{-10}$ of the intensity of the 19400 cm^{-1} laser line at 20 cm^{-1} from that line, less than 10^{-11} at greater than 65 cm^{-1}.
DISPERSION:	at 15802 cm^{-1} (He-Ne 6328A excitation) it is 11 cm^{-1}/mm.
RESOLUTION:	0.18 cm^{-1} at 17268 cm^{-1}, Order I (0.06A at 5791A, Order I)
SCANNING SPEED RANGE:	2-1000 cm^{-1}/min in 9 steps

No. 1454 SPECTROMETER-COUPLED RECORDER

An infrared compatible chart format is presented by coupling the stripchart recorder to the spectrometer drive. Chart the speed from 0-2000 cm^{-1} is 100 cm^{-1} per 2.5 cm and from 2000 to 4000, 200 cm^{-1} per 2.5 cm, regardless of scanning speed. Alternative scale expansions of 100, 40 and 20 cm^{-1} per 2.5 cm are provided as well.

When operated independently of the spectrometer the recorder chart can be driven synchronously at speeds variable from 0.25 to 10 cm per minute.

*Standard mirrors are aluminized. However, for a slight surcharge we can provide silvered mirrors which will increase the throughput of the spectrometer by a factor of 3/2. They are effective over the range 25000 cm^{-1} to 10000 cm^{-1} only and, therefore, are recommended in instruments which will be used exclusively for laser Raman spectroscopy with sources within that frequency range.

Digicat No. 1516

Di'gi-cat (dĭ' jĭ - kăt)

An electronic black box linking a Spex optical spectrometer with a computer for averaging out transients.

Although we do not honestly expect Webster's to become so unabridged as to catalog our new DIGICAT, we categorically expect the word to catch on as fast as the instrument's potentials are catalyzed.

With it you can

1. display wavelength remotely
2. scan at any of 15 speeds
3. rescan a fixed wavelength (CAT) from 2 to 999 times
4. jog one wavelength step at a time either manually or through your computer
5. tell the computer to study two preselected intervals

The DIGICAT generates command signals to Spex spectrometers equipped with stepper motor drive and optical shaft encoder. The stepper motor responds to command pulses and drives the spectrometer in a forward direction at any of 15 selectable step rates. The speed in terms of wavelength or wavenumber per second is dependent upon the step size (wavelength or wavenumber per step) selected on the gear box. Scanning in the reverse direction is available only at the maximum step rate. Of course the speed is again dependent on the gear setting. As well as issuing commands to the spectrometer, the DIGICAT displays the wavelength (or wavenumber or Δ wavenumber) to which the spectrometer is set.

The DIGICAT is commanded either by push-buttons on its front panel or by a computer to which it may be coupled directly; all input and output functions are available through TTL, 5V, positive logic signals with position information in BCD format.

Ramalog 4

offers:

TRIPLE MONOCHROMATOR FEATURES in a DOUBLE MONOCHROMATOR SYSTEM

YOUR CHOICE OF **1800 or 1200 g/mm gratings** for higher resolution or throughput

YOUR CHOICE OF
1- SYNCHRONOUS SCANNING
2- SIMPLE STEPPING SCANNING
3- "DIGICAT", SOPHISTICATED STEPPING/CATTING SCANNING

INFRARED COMPATIBLE RECORDING FORMAT

COLLECTING LENS IN SAMPLE ILLUMINATION SYSTEM with open end for unobstructed access

LASER BEAM EXPANDER

CLAASSEN FILTER for "cleaning" laser beam

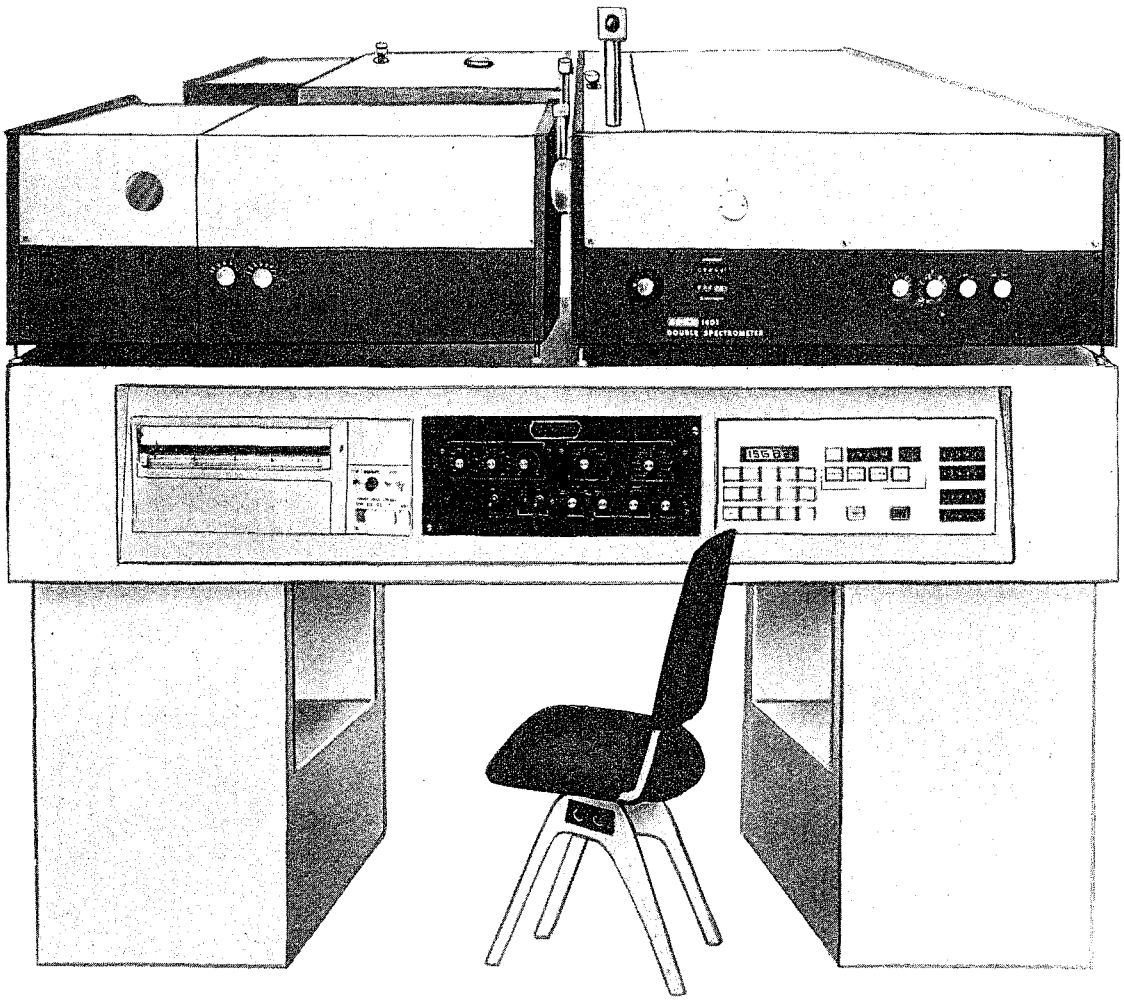

SPEX INDUSTRIES INC./P.O. BOX 798/METUCHEN, N.J. 08840

BULK RATE/U. S. POSTAGE
PAID
Permit No. 166/ Plainfield, N. J.